

Next to Soft Threshold Resummation for VH Production

Arunima Bhattacharya¹ Chinmoy Dey² M. C. Kumar² and Vaibhav Pandey²

¹ Theory Division, IFIC, University of Valencia-CSIC, E-46980 Paterna, Valencia, Spain

² Department of Physics, Indian Institute of Technology Guwahati, Guwahati-781039, Assam, India

Abstract. We study the threshold effects for the associated production of a Higgs boson with a massive vector boson ($V = Z, W$) in the $q\bar{q} \rightarrow V^* \rightarrow VH$ process at the LHC. By leveraging the universality of threshold logarithms and employing soft-virtual (SV) and next-to-soft virtual (NSV) resummation techniques, we compute threshold corrections to next-to-next-to-leading logarithmic accuracy. After matching the resummed predictions to the Next-to-Next-to-Leading order (NNLO) fixed order results, we present the invariant mass distribution to NNLO+ $\overline{\text{NNLL}}$ accuracy in QCD for the current LHC energies and the total production cross sections. The VH production channel is crucial for studying the couplings of the Higgs boson to the vector bosons (W, Z) and understanding the mechanism of electroweak symmetry breaking. Precision measurements of this process help test the validity of the standard model (SM) and can reveal potential deviations indicating new physics.

1 Introduction

Since its inception, the SM has satisfactorily explained many natural phenomena and made accurate predictions [1,2]. It also explains how fundamental particles gain mass by interacting with the Higgs field. Hence, the discovery of the Higgs boson on July 4, 2012, by the ATLAS and CMS collaborations at the Large Hadron Collider (LHC) [3,4] was a milestone achievement. Since then, the focus has shifted towards precise measurements of the Higgs boson's properties and interactions to test the robustness of the SM and probe potential signs of physics beyond the SM (BSM). However, the known SM falls short of explaining several observed phenomena, such as the baryon asymmetry of the universe, the nature of dark matter, or the tiny nonzero masses of neutrinos. Determining the CP properties of the Higgs boson is one of the many interests of various precision studies conducted worldwide. While current measurements indicate that it is a scalar with even parity [5,6], efforts continue scrutinising possible deviations. Additionally, numerous BSM theories predict new physics signatures that could subtly affect Higgs production and decay. Any discrepancies in measured cross sections or kinematic distributions for Higgs processes could serve as indirect evidence for such new physics [7,8,9,10,11,12,13,14,15,16].

In this context, the associated production of the Higgs boson with a massive vector boson (VH , where $V = Z, W^\pm$) is an important channel for probing Higgs boson

interactions and testing the SM's electroweak (EW) sector with high precision. The VH process is particularly valuable due to its sensitivity to the Higgs–vector boson coupling, enabling precise tests of the HVV vertex. Its experimental signatures are well-defined, especially in leptonic decay channels such as $W \rightarrow \ell\nu$ and $Z \rightarrow \ell^+\ell^-$, which provide clean final states with charged leptons and missing energy. These features facilitate event reconstruction and help suppress backgrounds, making the VH process an effective probe of Higgs properties. Although its cross section is smaller than that of gluon-gluon fusion (ggF) and vector boson fusion (VBF), the VH process remains a crucial avenue for precision Higgs studies [17,18,19,20,21]. Furthermore, VH production plays a pivotal role in Higgs decay analyses, particularly in the challenging $H \rightarrow b\bar{b}$ channel, and is instrumental in constraining the top-quark Yukawa coupling and its CP structure [7,8,9]. The presence of an accompanying vector boson enhances signal detection by mitigating QCD backgrounds, making this process a key focus of experimental efforts at ATLAS and CMS [17,18,22,19,20,21,23,24,25,26,27]. Complementing these experimental efforts, accurate theoretical predictions are essential for robust interpretations of Higgs measurements.

An important contribution to VH production arises from the gluon fusion channel [28,29,30], which, despite being a loop-induced process, provides non-negligible corrections. The leading-order (LO) ZH production subprocess has been computed with full top-quark mass effects in [28,29,31,32], showing a $\sim 7\%$ contribution relative to the next-to-leading order (NLO) Drell-Yan (DY)-type process, albeit with a substantial scale uncertainty of about 25%. In contrast, the next-to-next-to-leading order (N²LO) QCD DY-type correction contributes only about 3% relative to NLO. The effects of soft gluons in the $gg \rightarrow ZH$ subprocess have been studied for the total cross section at next-to-leading logarithmic (NLL) accuracy [30] and matched to NLO QCD in the effective field theory (EFT) approximation, yielding a correction of about 15%. Recently, invariant mass distributions for soft gluon resummation in gluon fusion ZH production have been presented in [33] at similar accuracy, further extended to next-to-soft effects.

Beyond fixed-order (FO) calculations, resummation techniques play a critical role in improving theoretical precision by systematically summing large threshold logarithms that arise near the partonic threshold. The resummation of these large threshold logarithms, specifically the soft-virtual (SV) corrections, is well-established in literature [34,35,36,37,38,39,40,41,42,43,44,45,46] and has been widely applied to various colorless processes [47,48,49,50,51,52,53,54,55,56,57,58,59,60,61,62,63,64,65,66]. These studies have shown improved predictions for inclusive cross sections and invariant mass distributions. For example, threshold resummation has been performed to next-to-next-to-next-to-leading logarithmic (N³LL) accuracy for ZH production *via* the DY-type channel and matched to N³LO QCD FO results [15]. These studies demonstrate improved perturbative convergence and reduced scale uncertainties, offering more reliable predictions for the invariant mass distribution of the ZH pair. Specifically, for the 13.6 TeV case, scale uncertainties decrease significantly from 4.06% at LO to 0.33% at N³LO, and from 4.44% at LO+LL to 0.58% at N³LO+N³LL. At this order the EW corrections are also important, the NLO EW correction for massive gauge bosons have been performed in [67,68,69,70,71,72,73,74,75], whereas the mixed EW correction are calculated in [76,77,78] and amount to -1.5% of NLO QCD in high invariant mass region. These findings emphasise the necessity of incorporating all relevant production channels to achieve precise theoretical predictions.

More recently, efforts have been made to incorporate next-to-soft (NSV) threshold effects as well [79,80,81,82,83,84,85,86,87,88,89,90,91,92,93,94,95,96,97,98,99,100]. Building upon these advancements, this work focuses on improving the predictions from [15] by incorporating next-to-soft virtual (NSV) threshold resummed corrections to next-to-next-to-leading logarithmic (NNLL) accuracy for the process $q\bar{q} \rightarrow V^* \rightarrow$

VH . By matching these results to NNLO FO calculations, we obtain high-precision predictions for the invariant mass distribution and total cross sections at LHC energies. These refined predictions provide essential theoretical support for Higgs precision physics, helping to identify potential deviations from the SM and offering valuable insights into possible new physics scenarios.

2 Theoretical Framework

The hadronic cross section for colorless production at the hadron collider is given by,

$$\sigma(Q^2) = \sum_{a,b=q,\bar{q},g} \int_0^1 dx_1 \int_0^1 dx_2 f_a(x_1, \mu_f^2) f_b(x_2, \mu_f^2) \int_0^1 dz \hat{\sigma}_{ab}(z, Q^2, \mu_f^2) \delta(\tau - zx_1x_2), \quad (1)$$

where $\sigma(Q^2) \equiv Q^2 d\sigma/dQ^2$ for the DY-type processes. To obtain the total production cross section of VH , we integrate over the invariant mass Q of the final VH state. The hadronic and partonic threshold variables τ and z are defined as

$$\tau = \frac{Q^2}{S}, \quad z = \frac{Q^2}{\hat{s}}, \quad (2)$$

where S and \hat{s} are the hadronic and partonic centre of mass energies, respectively. τ and z are thus related by $\tau = x_1x_2z$. The partonic coefficient $\hat{\sigma}_{ab}$ can be further decomposed as follows,

$$\hat{\sigma}_{ab}(z, Q^2, \mu_F^2) = \sigma^{(0)}(Q^2) \left[\Delta_{ab}^{\text{SV}}(z, \mu_f^2) + \Delta_{ab}^{\text{NSV}}(z, \mu_f^2) + \Delta_{ab}^{\text{hard}}(z, \mu_f^2) \right]. \quad (3)$$

where $\sigma^{(0)}$ represents the leading-order (LO) cross section, Δ_{ab}^{SV} represents the soft-virtual (SV) partonic coefficient and Δ_{ab}^{NSV} represents next-to soft-virtual (NSV) contributions. While Δ_{ab}^{SV} captures all the singular terms in the $z \rightarrow 1$ limit, Δ_{ab}^{NSV} contains contributions in the variable z , and $\Delta_{ab}^{\text{hard}}$ contains all regular terms in z . The SV+NSV cross section in z -space is computed in $d = 4 + \varepsilon$ dimensions using [92]

$$\Delta_{ab}(z, q^2, \mu_R^2, \mu_F^2) = \mathcal{C} \exp \{ \Psi_{ab}(z, q^2, \mu_R^2, \mu_F^2, \varepsilon) \} |_{\varepsilon=0} \quad (4)$$

where $\Psi_{ab}(z, q^2, \mu_R^2, \mu_F^2, \varepsilon)$ is a finite distribution and \mathcal{C} represents convolution. In order to study the all-order behaviour of the coefficient function Δ_{cc} , we move to Mellin (N-moment) space. In this N -moment space, it is convenient to use the following form of the partonic coefficient function for diagonal channel partonic processes:

$$\Delta_{cc,N}(q^2, \mu_R^2, \mu_F^2) = C_0(q^2, \mu_R^2, \mu_F^2) \exp(\Psi_N^c(q^2, \mu_F^2)), \quad (5)$$

A detailed study of this structuring is done in [92]. The coefficient $C_0(q^2, \mu_R^2, \mu_F^2)$ contains all the process-dependent information and is independent of the Mellin moment. $C_0(q^2, \mu_R^2, \mu_F^2)$ can be expanded in powers of $a_s(\mu_R^2)$ as

$$C_0^g(q^2, \mu_R^2, \mu_F^2) = \sum_{i=0}^{\infty} a_s^i(\mu_R^2) C_{0i}^g(q^2, \mu_R^2, \mu_F^2), \quad (6)$$

where the coefficients C_{0i}^g for VH production ($V = Z, W$) are given in [15]. Here $a_s = \alpha_s/(4\pi)$, where α_s is the strong coupling constant. The term inside the exponential depends on the initial channel of the process under study and can be expressed as

$$\Psi_{\mathcal{D}}^{cc} = \Psi_{\text{SV,N}}^{cc} + \Psi_{\text{NSV,N}}^{cc}, \quad (7)$$

where we can split Ψ_D^{cc} in such a way that all those terms that are functions of $\log^j(N)$, $j = 0, 1, \dots$ are kept in $\Psi_{SV,N}^{cc}$ and the remaining terms that are proportional to $(1/N)\log^j(N)$, $j = 0, 1, \dots$ are contained in $\Psi_{NSV,N}^{cc}$. These coefficients solely depend on the initial state partons, which for the process under study is $q\bar{q}$. Following the formalism in [92], the $\Psi_{SV,N}^{cc}$ and $\Psi_{NSV,N}^{cc}$ to all orders can be written as,

$$\Psi_{SV,N}^{cc} = \log(g_0^c(a_s(\mu_R^2))) + g_1^c(\omega) \log(N) + \sum_{i=0}^{\infty} a_s^i(\mu_R^2) g_{i+2}^c(\omega), \quad (8)$$

$$\Psi_{NSV,N}^{cc} = \frac{1}{N} \sum_{i=0}^{\infty} a_s^i(\mu_R^2) \left(\bar{g}_{i+1}^c(\omega) + h_i^c(\omega, N) \right). \quad (9)$$

The resummation constants g_i , \bar{g}_i and h_i are available for gluon fusion and quark-antiquark annihilation initiated channels in [92,35,39,58].

The resummed results have been matched with the available FO results to incorporate the hard regular contribution and, simultaneously, avoid double counting of SV (NSV) logarithms. The matching with the FO is performed using the *minimal prescription* [101] and for \overline{NnLL} resummation it reads,

$$Q^2 \frac{d\sigma_{ab}^{NnLO+\overline{NnLL}}}{dQ^2} = Q^2 \frac{d\sigma_{ab}^{NnLO}}{dQ^2} + \sum_{ab \in \{gg, q\bar{q}\}} \hat{\sigma}_{ab}^{(0)}(Q^2) \int_{c-i\infty}^{c+i\infty} \frac{dN}{2\pi i} \tau^{-N} f_{a,N}(\mu_f) f_{b,N}(\mu_f) \quad (10)$$

$$\times \left(Q^2 \frac{d\hat{\sigma}_{N,ab}^{\overline{NnLL}}}{dQ^2} - Q^2 \frac{d\hat{\sigma}_{N,ab}^{\overline{NnLL}}}{dQ^2} \Big|_{\text{tr}} \right). \quad (11)$$

In the later sections, we present these matched results in the \overline{N} -scheme ($\overline{N} = Ne^{\gamma_E}$, where γ_E is the Euler–Mascheroni constant) following the approach given in [63]. We also define K-factors for the FO (K_{nm}), SV resummed (R_{nm}) and NSV resummed (\overline{R}_{nm}) cross sections as below:

$$K_{nm} = \frac{\sigma^{NnLO}}{\sigma_c^{NnLO}}, R_{nm} = \frac{\sigma^{NnLO+NnLL}}{\sigma_c^{NnLO}} \text{ and } \overline{R}_{nm} = \frac{\sigma^{NnLO+\overline{NnLL}}}{\sigma_c^{NnLO}}. \quad (12)$$

Using these tools and methodologies, we have calculated the invariant mass-distribution, 7-point scale uncertainties, PDF intrinsic uncertainties, scale uncertainties and the total production cross sections for $q\bar{q} \rightarrow V^* \rightarrow VH$. These results are discussed in the next section of the article.

3 Results and Discussion

For the numerical evaluations we use the EW couplings in G_μ scheme, where we use $G_F = 1.1663788 \times 10^{-5}$, $m_Z = 91.1880$ GeV and $m_W = 80.3692$ GeV to calculate the fine structure constant $\alpha = G_F(8 \sin^2 \theta_W \cos^2 \theta_W m_Z^2)/(4\sqrt{2}\pi)$ with $\cos^2 \theta_W = m_W^2/m_Z^2$. The decay widths are taken to be $\Gamma_Z = 2.4955$ GeV and $\Gamma_W = 2.085$ GeV. The mass of the Higgs boson is taken to be $m_H = 125.2$ GeV. Our calculations are done with five massless quark flavours ($n_f = 5$). In our calculation, the CKM matrix elements are $V_{ud} = 0.97446$, $V_{us} = 0.22452$, $V_{ub} = 0.00365$, $V_{cd} = 0.22438$,

$V_{cs} = 0.97359$ and $V_{cb} = 0.04214$. The partonic cross sections are folded with the MSHT20 [102] sets of parton distribution functions (PDFs) extracted at NNLO level, and the strong coupling constant is taken from LHAPDF [103] with $\alpha_s(m_Z) = 0.118$. The central choice of scale for the unphysical renormalization and factorization scales is taken to be the invariant mass Q of the VH final state ($\mu_R = \mu_F = Q$). The conventional 7-point scale variation is performed by varying the unphysical scales in the range such that $|\ln(\mu_R/\mu_F)| \leq \ln 2$.

We utilise `n3loxs` package to compute the FO results for neutral and charged DY type VH production process [104,105]. At the NNLO level for the ZH production process, in addition to the quark annihilation process, there will also be contributions coming the loop induced gluon fusion channel and top-quark loops. Apart from these, there will also contribution from the bottom annihilation process where the Higgs boson directly couples to the bottom quark. We have taken all these contributions from `vh@nnlo` [106,107].

In fig. 1, fig. 2 and fig. 3, we present the invariant mass distribution for the ZH and $W^\pm H$ production processes up to NNLO+NNLL accuracy from 250 GeV to 3000 GeV at 13.6 TeV LHC. The cross section decreases with the diminution of the $q\bar{q}$ flux from the low to the high Q region. To understand the importance of these corrections better, the corresponding K-factors (defined in eq. 12) are shown in the lower panel of the same plots. The fixed order K-factors K_{10} and K_{20} for ZH production acquire values of up to 1.30 and 1.36, respectively, in the high Q region around 3 TeV. In the same Q range, the K-factors associated with the SV resummed corrections, namely R_{10} and R_{20} , reach approximately 1.37 and 1.38. Furthermore, the inclusion of NSV logarithms increase the K-factors, \bar{R}_{10} and \bar{R}_{20} , to approximately 1.40 and 1.38, respectively. A comparable pattern is observed for charged DY processes, where the NLO K-factor (K_{10}) and the NNLO K-factor (K_{20}) undergo substantial modifications upon incorporating the resummed results to NLO+NLL (\bar{R}_{10}) and NNLO+NNLL (\bar{R}_{20}) accuracy. A key observation in figs. 1, 2 and 3 is that the addition of NSV resummation to the SV resummed results at two-loop order negatively impacts the K-factor values, denoted by R_{20} and \bar{R}_{20} . This can be attributed to our choice of working in the \bar{N} scheme. To understand this interplay between schemes, check [108] where the authors present the resummed predictions for inclusive cross section for DY production. In fig. 14 of [108], the NLO + NLL results are shown to be overestimated in the \bar{N} -scheme compared to the ones in the N -scheme. The same figure also illustrates that the results at two-loop accuracy (NNLO + NNLL) in both the schemes are comparable. This indicates a decrease in values from the NLO + NLL results in the \bar{N} -scheme, while showing an increase in values in the N -scheme. It is also worth noting that the rate of convergence of the perturbation series is better for \bar{N} -scheme compared to N -scheme in Ref. [63].

Fig. 4 depicts the 7-point scale uncertainties for ZH and $W^\pm H$ production processes at NNLO, NNLO+NNLL, and NNLO+NNLL accuracy, ranging from 250 GeV to 3000 GeV at the 13.6 TeV LHC. In the low Q region (< 900 GeV), the uncertainties increase as we move from NNLO to NNLO+NNLL and then to NNLO+NNLL. On the other hand, in the high Q region, the SV resummed corrections reduce the scale uncertainties compared to the FO results. Conversely, the NSV resummed corrections demonstrate higher uncertainties than NNLO and NNLO+NNLL. To understand this behaviour, we need to recollect that for VH production, apart from the $q\bar{q}$ initiated sub-process, we have contributions from other partonic channels like qg and gg . However, in this work, we are focusing on the threshold resummation for the $q\bar{q}$ channel only. The other parton channels (e.g. qg) will not contribute to the threshold (SV) logarithms. However, such channels do contribute to the NSV logarithms and are not

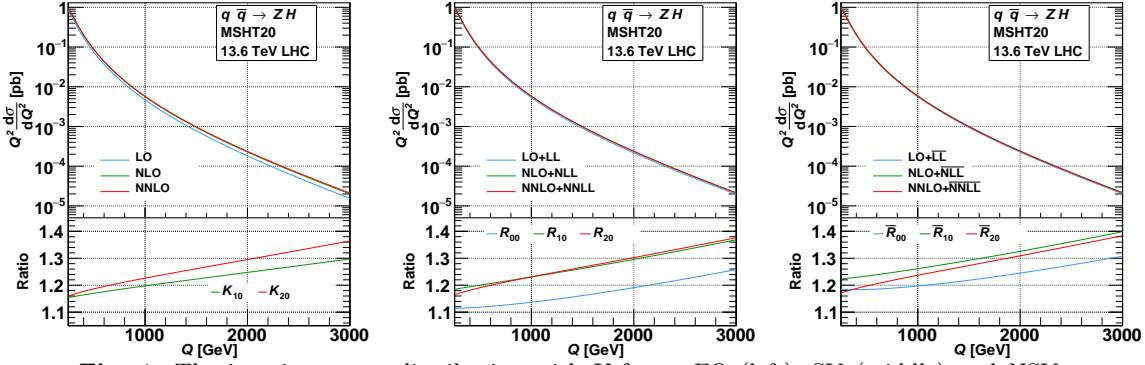


Fig. 1. The invariant mass distribution with K-factor FO (left), SV (middle) and NSV (right) are shown for the $q\bar{q} \rightarrow ZH$ process at 13.6 TeV LHC.

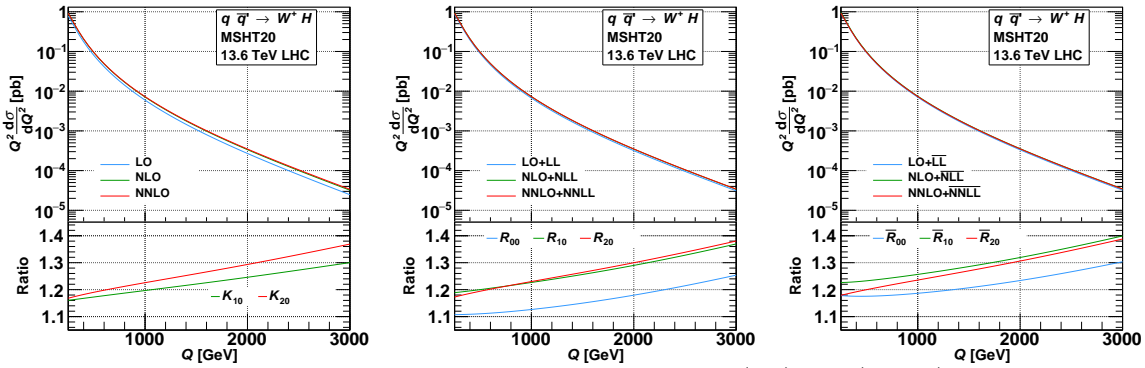


Fig. 2. The invariant mass distribution with K-factor FO (left), SV (middle) and NSV (right) are shown for the $q\bar{q}' \rightarrow W^+H$ process at 13.6 TeV LHC.

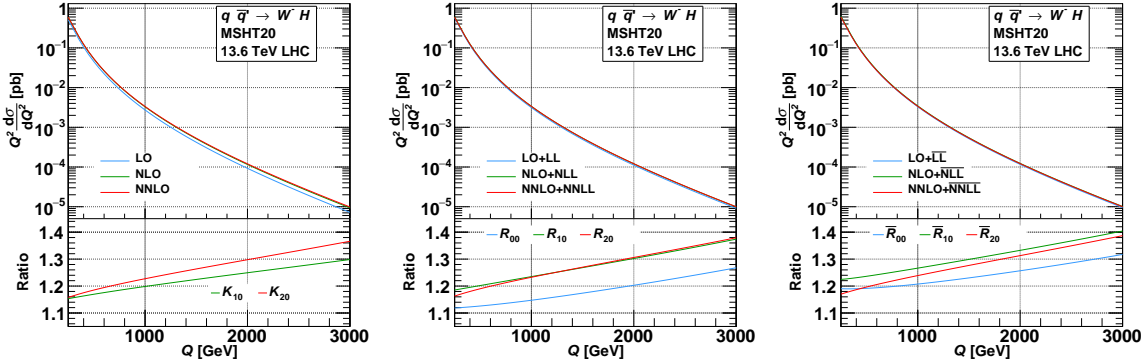


Fig. 3. The invariant mass distribution with K-factor FO (left), SV (middle) and NSV (right) are shown for the $q\bar{q}' \rightarrow W^-H$ process at 13.6 TeV LHC.

considered in the present work. Therefore, we observe that incorporating the NSV resummation leads to an increase in scale uncertainties.

For completeness, we study the scale variations due to μ_R and μ_F separately by varying one and keeping the other fixed at Q . Fig. 5 and fig. 6 depicts the renormalisation scale (μ_R) and factorization scale (μ_F) uncertainties, respectively. These results follow a similar behavior as the 7-point scale uncertainty results. To gain a better understanding, we analyse the results from the $q\bar{q}$ channel alone at NNLO,

NNLO+NNLL, and NNLO+ $\overline{\text{NNLL}}$, as shown in fig. 7, focusing on the variation of the μ_R scale. We observe a significant reduction in the percentage of uncertainty as we move from NNLO to NNLO+NNLL and then to NNLO+ $\overline{\text{NNLL}}$. Specifically, the percentage of uncertainty decreases from 0.25 to 0.10 in the high Q region, as expected.

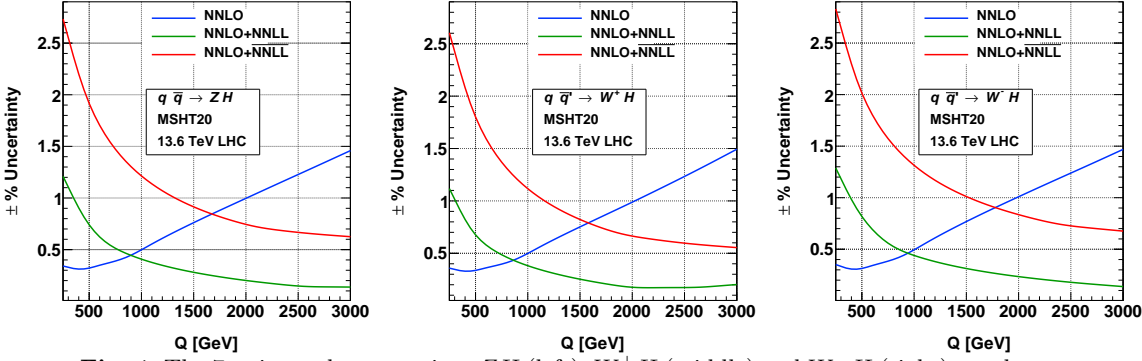


Fig. 4. The 7-point scale uncertainty ZH (left), W^+H (middle) and W^-H (right) are shown at 13.6 TeV LHC.

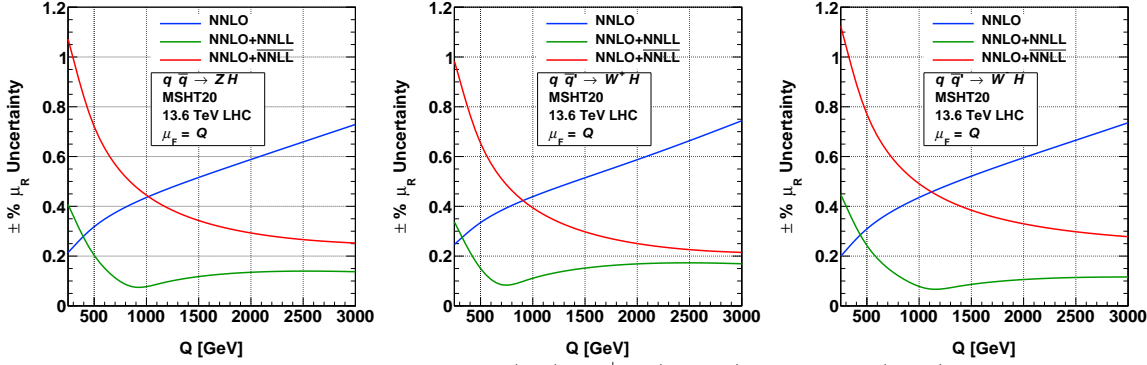


Fig. 5. The μ_R scale uncertainty ZH (left), W^+H (middle) and W^-H (right) are shown at 13.6 TeV LHC.

We also study the intrinsic PDF uncertainties by calculating the NNLO+ $\overline{\text{NNLL}}$ cross section using 64 different sets of MSHT20 PDFs. For this analysis, we utilise LHAPDF routines. The results are illustrated in fig. 8, showing that the uncertainties can reach up to 5% in the 3 TeV range.

Finally, in tables 1, 2, and 3, we present the total production cross sections for the VH production processes at NNLO, NNLO+NNLL, and NNLO+ $\overline{\text{NNLL}}$ for center-of-mass energies of 13 TeV, 13.6 TeV and 100 TeV. In the present context, we consider all these three contributions to the ZH production process and define the total production cross section as

$$\sigma_{tot,ZH}^{\text{NNLO}} = \sigma_{\text{DY},ZH}^{\text{NNLO}} + \sigma^{gg}(a_s^2) + \sigma^{\text{top}}(a_s^2) + \sigma^{b\bar{b}} \quad (13)$$

$$\sigma_{tot,ZH}^{\text{NNLO+NNLL}} = \sigma_{\text{DY},ZH}^{\text{NNLO+NNLL}} + \sigma^{gg}(a_s^2) + \sigma^{\text{top}}(a_s^2) + \sigma^{b\bar{b}} \quad (14)$$

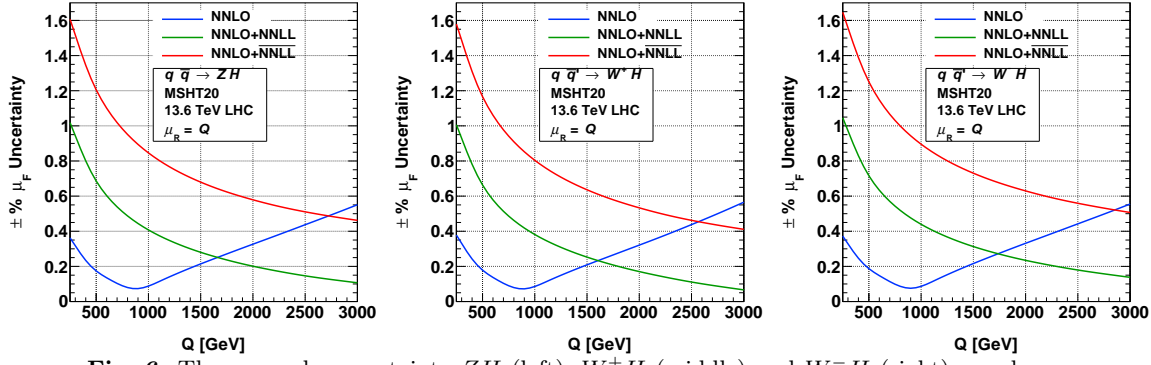


Fig. 6. The μ_F scale uncertainty ZH (left), W^+H (middle) and W^-H (right) are shown at 13.6 TeV LHC.

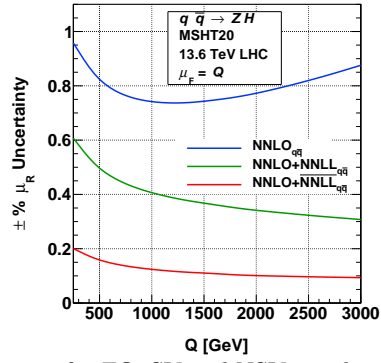


Fig. 7. The μ_R scale uncertainty for FO, SV and NSV are shown for only $q\bar{q} \rightarrow ZH$ process at 13.6 TeV LHC.

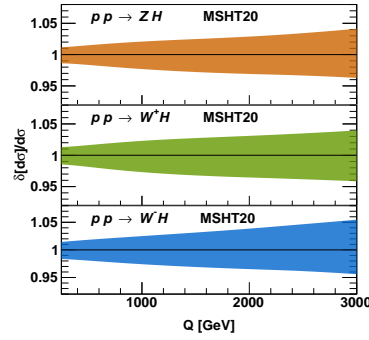


Fig. 8. The PDF uncertainty are shown for the $pp \rightarrow VH$ process at NNLO+NNLL for 13.6 TeV LHC.

$$\sigma_{tot,ZH}^{\text{NNLO+NNLL}} = \sigma_{\text{DY,ZH}}^{\text{NNLO+NNLL}} + \sigma^{gg}(a_s^2) + \sigma^{\text{top}}(a_s^2) + \sigma^{b\bar{b}} \quad (15)$$

For the case of WH production process, we define the total production cross section as

$$\sigma_{tot,WH}^{\text{NNLO}} = \sigma_{\text{DY,WH}}^{\text{NNLO}} + \sigma^{\text{top}}(a_s^2) \quad (16)$$

$$\sigma_{tot,WH}^{\text{NNLO+NNLL}} = \sigma_{\text{DY,WH}}^{\text{NNLO+NNLL}} + \sigma^{\text{top}}(a_s^2). \quad (17)$$

Order	13 TeV	13.6 TeV	100 TeV
$\sigma_{tot,ZH}^{\text{NNLO}}$	$0.8566 \pm 1.64\%$	$0.9130 \pm 1.66\%$	$11.3200 \pm 3.64\%$
$\sigma_{tot,ZH}^{\text{NNLO}+\text{NNLL}}$	$0.8597 \pm 0.91\%$	$0.9163 \pm 0.94\%$	$11.3475 \pm 2.41\%$
$\sigma_{tot,ZH}^{\text{NNLO}+\overline{\text{NNLL}}}$	$0.8644 \pm 2.17\%$	$0.9212 \pm 2.12\%$	$11.3923 \pm 1.61\%$

Table 1. The ZH production cross sections (in pb) are presented along with corresponding FO, SV and NSV resummed results at different center of mass energy with 7-point scale uncertainties.

Order	13 TeV	13.6 TeV	100 TeV
$\sigma_{tot,W^+H}^{\text{NNLO}}$	$0.9031 \pm 0.43\%$	$0.9554 \pm 0.43\%$	$8.8276 \pm 1.11\%$
$\sigma_{tot,W^+H}^{\text{NNLO}+\text{NNLL}}$	$0.9063 \pm 1.23\%$	$0.9588 \pm 1.23\%$	$8.8525 \pm 1.72\%$
$\sigma_{tot,W^+H}^{\text{NNLO}+\overline{\text{NNLL}}}$	$0.9112 \pm 3.12\%$	$0.9640 \pm 3.12\%$	$8.8917 \pm 2.89\%$

Table 2. The W^+H production cross sections (in pb) are presented along with corresponding FO, SV and NSV resummed results at different center of mass energy with 7-point scale uncertainties.

Order	13 TeV	13.6 TeV	100 TeV
$\sigma_{tot,W^-H}^{\text{NNLO}}$	$0.5686 \pm 0.48\%$	$0.6063 \pm 0.48\%$	$7.0340 \pm 1.10\%$
$\sigma_{tot,W^-H}^{\text{NNLO}+\text{NNLL}}$	$0.5710 \pm 1.25\%$	$0.6088 \pm 1.25\%$	$7.0552 \pm 1.41\%$
$\sigma_{tot,W^-H}^{\text{NNLO}+\overline{\text{NNLL}}}$	$0.5744 \pm 3.32\%$	$0.6125 \pm 3.32\%$	$7.0899 \pm 3.01\%$

Table 3. The W^-H production cross sections (in pb) are presented along with corresponding FO, SV and NSV resummed results at different center of mass energy with 7-point scale uncertainties.

$$\sigma_{tot,WH}^{\text{NNLO}+\overline{\text{NNLL}}} = \sigma_{\text{DY},WH}^{\text{NNLO}+\overline{\text{NNLL}}} + \sigma^{\text{top}}(a_s^2). \quad (18)$$

At 13.6 TeV, the SV resummed results enhance the NNLO ZH production cross section by 0.37%, while the NSV results lead to an additional enhancement of 0.53%. For W^+H production, the enhancement is 0.36% from NNLO to NNLO+NNLL and 0.54% from NNLO+NNLL to NNLO+ $\overline{\text{NNLL}}$. In the case of W^-H , the SV resummed results show a 0.40% enhancement over the NNLO value, and the NSV resummed results provide a further 0.61% increase compared to the SV results. Consequently, the inclusion of NSV logarithms results in corrections of approximately 0.89% for ZH production, 0.90% for W^+H production, and 1.02% for W^-H production compared to the NNLO results at a center-of-mass energy of 13.6 TeV at the LHC. We also observe that the cross sections in general increase with increases in the center of mass energy due to the enhancement of available parton fluxes.

4 Conclusions

In this work, we have investigated the impact of next-to-soft (NSV) threshold resummation on associated Higgs production with a vector boson (VH , where $V = Z, W^\pm$), a crucial process in the Higgs precision program at the LHC. By performing resummation at NNLL accuracy and matching our results with FO NNLO calculations, we

provide precise predictions for the invariant mass distribution at 13.6 TeV and total production cross sections at 13, 13.6, and 100 TeV.

The precise computation of threshold corrections continues to be an area of significant theoretical interest, particularly in understanding the role of NSV effects and their factorisation properties [109,110,94,85]. In this study, we employ the generic resummation approach developed in [95,92] to systematically compute both SV and NSV resummed corrections to $q\bar{q} \rightarrow VH$ production at two-loop accuracy. The foundation of our work lies in the observation that for diagonal channels, the SV+NSV resummed structure depends solely on the initial parton channels, and the process-dependent information is encapsulated in the coefficient C_0 of eqn. 5. This framework validated up to NNLO for Higgs and DY production [92,95,111,46,108,93,112] is applied here to a $2 \rightarrow 2$ process of form factor-type diagrams, demonstrating results that align with theoretical expectations. We observe that in the high- Q region, the NSV resummation contributes an additional 2% of the LO to the NNLO results and further, it reduces the μ_R scale uncertainty from 0.25% to 0.10% in the high Q region for the $q\bar{q}$ -channel. Given the increasing demand for high-precision theoretical predictions in upcoming LHC runs and future collider experiments, the results provided in this work pave the way for their broader application in Higgs phenomenology and beyond. These refined predictions significantly enhance the reliability of theoretical calculations, facilitating more accurate extractions of Higgs couplings from experimental data. These developments will be instrumental in probing potential deviations from the SM and exploring new physics scenarios with greater sensitivity.

A.B. acknowledge the financial support by the Generalitat Valenciana, the spanish government and ERDF funds from the European Commission (CNS2022-136165, funded by MCIN/AEI/10.13039/501100011033/ and by the European Union “NextGenerationEU/PRTR”). The research work of M.C.K. is supported by the SERB Core Research Grant (CRG) under the project CRG/2021/005270.

References

1. ATLAS Collaboration. A detailed map of higgs boson interactions by the atlas experiment ten years after the discovery. *Nature*, 607:52–59, 2022.
2. CMS Collaboration. A portrait of the higgs boson by the cms experiment ten years after the discovery. *Nature*, 607:60–68, 2022.
3. Georges Aad et al. Observation of a new particle in the search for the Standard Model Higgs boson with the ATLAS detector at the LHC. *Phys. Lett. B*, 716:1–29, 2012.
4. Serguei Chatrchyan et al. Observation of a New Boson at a Mass of 125 GeV with the CMS Experiment at the LHC. *Phys. Lett. B*, 716:30–61, 2012.
5. Albert M Sirunyan et al. Constraints on anomalous Higgs boson couplings using production and decay information in the four-lepton final state. *Phys. Lett. B*, 775:1–24, 2017.
6. Morad Aaboud et al. Measurement of the Higgs boson coupling properties in the $H \rightarrow ZZ^* \rightarrow 4\ell$ decay channel at $\sqrt{s} = 13$ TeV with the ATLAS detector. *JHEP*, 03:095, 2018.
7. Christoph Englert, Matthew McCullough, and Michael Spannowsky. Gluon-initiated associated production boosts Higgs physics. *Phys. Rev. D*, 89(1):013013, 2014.
8. B. Hespel, F. Maltoni, and E. Vryonidou. Higgs and Z boson associated production via gluon fusion in the SM and the 2HDM. *JHEP*, 06:065, 2015.
9. Dorival Goncalves, Frank Krauss, Silvan Kuttimalai, and Philipp Maierhöfer. Higgs-Strahlung: Merging the NLO Drell-Yan and Loop-Induced 0+1 jet Multiplicities. *Phys. Rev. D*, 92(7):073006, 2015.

10. Arunima Bhattacharya, Maguni Mahakhud, Prakash Mathews, and V. Ravindran. Two loop QCD amplitudes for di-pseudo scalar production in gluon fusion. *JHEP*, 02:121, 2020.
11. Arunima Bhattacharya, M. C. Kumar, Prakash Mathews, and V. Ravindran. Next-to-soft-virtual resummed prediction for pseudoscalar Higgs boson production at NNLO+NNLL⁻. *Phys. Rev. D*, 105(11):116015, 2022.
12. J. Baglio, F. Campanario, S. Glaus, M. Mühlleitner, J. Ronca, and M. Spira. Full NLO QCD predictions for Higgs-pair production in the 2-Higgs-doublet model. *Eur. Phys. J. C*, 83(9):826, 2023.
13. Syuhei Iguro, Teppei Kitahara, Yuji Omura, and Hantian Zhang. Chasing the two-Higgs doublet model in the di-Higgs boson production. *Phys. Rev. D*, 107(7):075017, 2023.
14. Taushif Ahmed, V. Ravindran, Aparna Sankar, and Surabhi Tiwari. Two-loop amplitudes for di-Higgs and di-pseudo-Higgs productions through quark annihilation in QCD. *JHEP*, 01:189, 2022.
15. Goutam Das, Chinmoy Dey, M. C. Kumar, and Kajal Samanta. Threshold enhanced cross sections for colorless productions. *Phys. Rev. D*, 107(3):034038, 2023.
16. Pulak Banerjee, Chinmoy Dey, M. C. Kumar, and V. Ravindran. Pseudo-scalar Higgs decay to three parton amplitudes at NNLO to higher orders in dimensional regulator. 11 2024.
17. Morad Aaboud et al. Measurement of VH , $H \rightarrow b\bar{b}$ production as a function of the vector-boson transverse momentum in 13 TeV pp collisions with the ATLAS detector. *JHEP*, 05:141, 2019.
18. Georges Aad et al. Measurement of the associated production of a Higgs boson decaying into b -quarks with a vector boson at high transverse momentum in pp collisions at $\sqrt{s} = 13$ TeV with the ATLAS detector. *Phys. Lett. B*, 816:136204, 2021.
19. Combined Higgs boson production and decay measurements with up to 137 fb^{-1} of proton-proton collision data at $\sqrt{s} = 13$ TeV. 2020.
20. Combination of measurements of Higgs boson production in association with a W or Z boson in the $b\bar{b}$ decay channel with the ATLAS experiment at $\sqrt{s} = 13$ TeV. 2021.
21. Vladimir Chekhovsky et al. Constraints on standard model effective field theory for a Higgs boson produced in association with W or Z bosons in the $H \rightarrow b\bar{b}$ decay channel in proton-proton collisions at $\sqrt{s} = 13$ TeV. 11 2024.
22. Georges Aad et al. Measurements of WH and ZH production in the $H \rightarrow b\bar{b}$ decay channel in pp collisions at 13 TeV with the ATLAS detector. *Eur. Phys. J. C*, 81(2):178, 2021.
23. Aram Hayrapetyan et al. Study of WH production through vector boson scattering and extraction of the relative sign of the W and Z couplings to the Higgs boson in proton-proton collisions at $\sqrt{s} = 13$ TeV. 5 2024.
24. Aram Hayrapetyan et al. Search for ZZ and ZH production in the $b\bar{b}b\bar{b}$ final state using proton-proton collisions at $\sqrt{s} = 13$ TeV. *Eur. Phys. J. C*, 84(7):712, 2024.
25. Aram Hayrapetyan et al. Search for Higgs boson pair production with one associated vector boson in proton-proton collisions at $\sqrt{s} = 13$ TeV. *JHEP*, 10:061, 2024.
26. Armen Tumasyan et al. Measurement of simplified template cross sections of the Higgs boson produced in association with W or Z bosons in the $H \rightarrow b\bar{b}$ decay channel in proton-proton collisions at $s=13$ TeV. *Phys. Rev. D*, 109(9):092011, 2024.
27. Georges Aad et al. Measurements of WH and ZH production with Higgs boson decays into bottom quarks and direct constraints on the charm Yukawa coupling in 13 TeV pp collisions with the ATLAS detector. 10 2024.
28. Duane A. Dicus and Chung Kao. Higgs Boson - Z^0 Production From Gluon Fusion. *Phys. Rev. D*, 38:1008, 1988. [Erratum: *Phys.Rev.D* 42, 2412 (1990)].
29. Bernd A. Kniehl and Caesar P. Palisoc. Associated production of Z and neutral Higgs bosons at the CERN Large Hadron Collider. *Phys. Rev. D*, 85:075027, 2012.
30. Robert V. Harlander, Anna Kulesza, Vincent Theeuwes, and Tom Zirke. Soft gluon resummation for gluon-induced Higgs Strahlung. *JHEP*, 11:082, 2014.

31. Bernd A. Kniehl. Associated Production of Higgs and Z Bosons From Gluon Fusion in Hadron Collisions. *Phys. Rev. D*, 42:2253–2258, 1990.
32. Bernd A. Kniehl. On the Decay Mode $Z \rightarrow H gg$. *Phys. Rev. D*, 42:3100–3106, 1990.
33. Goutam Das, Chinmoy Dey, M. C. Kumar, and Kajal Samanta. Soft gluon resummation for gluon fusion ZH production. 1 2025.
34. George F. Sterman. Summation of Large Corrections to Short Distance Hadronic Cross-Sections. *Nucl. Phys. B*, 281:310–364, 1987.
35. S. Catani and L. Trentadue. Resummation of the QCD Perturbative Series for Hard Processes. *Nucl. Phys. B*, 327:323–352, 1989.
36. S. Catani and L. Trentadue. Comment on QCD exponentiation at large x . *Nucl. Phys. B*, 353:183–186, 1991.
37. Nikolaos Kidonakis and George Sterman. Resummation for qcd hard scattering. *Nucl. Phys. B*, 505:321–348, 1997.
38. Nikolaos Kidonakis. A unified approach to nlo soft and virtual corrections in electroweak, higgs, qcd, and susy processes. *Int. J. Mod. Phys. A*, 19:1793–1804, 2004.
39. S. Moch, J. A. M. Vermaseren, and A. Vogt. Higher-order corrections in threshold resummation. *Nucl. Phys. B*, 726:317–335, 2005.
40. Eric Laenen and Lorenzo Magnea. Threshold resummation for electroweak annihilation from DIS data. *Phys. Lett. B*, 632:270–276, 2006.
41. Nikolaos Kidonakis. Next-to-next-to-next-to-leading-order soft-gluon corrections in hard-scattering processes near threshold. *Phys. Rev. D*, 73:034001, 2006.
42. V. Ravindran. On Sudakov and soft resummations in QCD. *Nucl. Phys. B*, 746:58–76, 2006.
43. V. Ravindran. Higher-order threshold effects to inclusive processes in QCD. *Nucl. Phys. B*, 752:173–196, 2006.
44. Ahmad Idilbi, Xiang-dong Ji, and Feng Yuan. Resummation of threshold logarithms in effective field theory for DIS, Drell-Yan and Higgs production. *Nucl. Phys. B*, 753:42–68, 2006.
45. Thomas Becher, Matthias Neubert, and Ben D. Pecjak. Factorization and Momentum-Space Resummation in Deep-Inelastic Scattering. *JHEP*, 01:076, 2007.
46. Taushif Ahmed, A. H. Ajjath, Goutam Das, Pooja Mukherjee, V. Ravindran, and Surabhi Tiwari. Soft-virtual correction and threshold resummation for n -colorless particles to fourth order in QCD: Part I. 10 2020.
47. Stefano Catani, Daniel de Florian, Massimiliano Grazzini, and Paolo Nason. Soft gluon resummation for Higgs boson production at hadron colliders. *JHEP*, 07:028, 2003.
48. S. Moch and A. Vogt. Higher-order soft corrections to lepton pair and Higgs boson production. *Phys. Lett. B*, 631:48–57, 2005.
49. Daniel de Florian and Jose Zurita. Soft-gluon resummation for pseudoscalar Higgs boson production at hadron colliders. *Phys. Lett. B*, 659:813–820, 2008.
50. Nikolaos Kidonakis. Collinear and soft-gluon corrections to higgs production at next-to-next-to-next-to-leading order. *Phys. Rev. D*, 77:053008, 2008.
51. Stefano Catani, Leandro Cieri, Daniel de Florian, Giancarlo Ferrera, and Massimiliano Grazzini. Threshold resummation at N^3LL accuracy and soft-virtual cross sections at N^3LO . *Nucl. Phys. B*, 888:75–91, 2014.
52. Marco Bonvini and Simone Marzani. Resummed Higgs cross section at N^3LL . *JHEP*, 09:007, 2014.
53. Taushif Ahmed, Goutam Das, M. C. Kumar, Narayan Rana, and V. Ravindran. RG improved Higgs boson production to N^3LO in QCD. 5 2015.
54. Timo Schmidt and Michael Spira. Higgs Boson Production via Gluon Fusion: Soft-Gluon Resummation including Mass Effects. *Phys. Rev. D*, 93(1):014022, 2016.
55. Taushif Ahmed, Marco Bonvini, M. C. Kumar, Prakash Mathews, Narayan Rana, V. Ravindran, and Luca Rottoli. Pseudo-scalar Higgs boson production at $N^3 LO_A + N^3 LL'$. *Eur. Phys. J. C*, 76(12):663, 2016.
56. Marco Bonvini, Simone Marzani, Claudio Muselli, and Luca Rottoli. On the Higgs cross section at $N^3LO + N^3LL$ and its uncertainty. *JHEP*, 08:105, 2016.

57. Nikolaos Kidonakis. Higher-order radiative corrections for $b\bar{b} \rightarrow H^- W^+$. *Phys. Rev. D*, 97(3):034002, 2018.
58. Ajjath A H, Amlan Chakraborty, Goutam Das, Pooja Mukherjee, and V. Ravindran. Resummed prediction for Higgs boson production through $b\bar{b}$ annihilation at N³LL. *JHEP*, 11:006, 2019.
59. Goutam Das, Sven-Olaf Moch, and Andreas Vogt. Soft corrections to inclusive deep-inelastic scattering at four loops and beyond. *JHEP*, 03:116, 2020.
60. Goutam Das, M. C. Kumar, and Kajal Samanta. Resummed inclusive cross-section in ADD model at N³LL. *JHEP*, 10:161, 2020.
61. Goutam Das, M. C. Kumar, and Kajal Samanta. Resummed inclusive cross-section in Randall-Sundrum model at NNLO+NNLL. *JHEP*, 07:040, 2020.
62. Goutam Das, M. C. Kumar, and Kajal Samanta. Precision QCD phenomenology of exotic spin-2 search at the LHC. *JHEP*, 04:111, 2021.
63. Ajjath A H, Goutam Das, M. C. Kumar, Pooja Mukherjee, V. Ravindran, and Kajal Samanta. Resummed Drell-Yan cross-section at N³LL. *JHEP*, 10:153, 2020.
64. Ajjath A H and Hua-Sheng Shao. N³LO+N³LL QCD improved Higgs pair cross sections. *JHEP*, 02:067, 2023.
65. Goutam Das, Chinmoy Dey, M. C. Kumar, and Kajal Samanta. Precision Studies for Higgs-Strahlung Process at Hadron Collider. *Springer Proc. Phys.*, 304:245–249, 2024.
66. Pulak Banerjee, Chinmoy Dey, M. C. Kumar, and Vaibhav Pandey. Threshold resummation for Z-boson pair production at NNLO+NNLL. 9 2024.
67. Stefan Dittmaier and Michael Krämer. Electroweak radiative corrections to W boson production at hadron colliders. *Phys. Rev. D*, 65:073007, 2002.
68. U. Baur, O. Brein, W. Hollik, C. Schappacher, and D. Wackerth. Electroweak radiative corrections to neutral current Drell-Yan processes at hadron colliders. *Phys. Rev. D*, 65:033007, 2002.
69. U. Baur and D. Wackerth. Electroweak radiative corrections to $p\bar{p} \rightarrow W^\pm \rightarrow \ell^\pm \nu$ beyond the pole approximation. *Phys. Rev. D*, 70:073015, 2004.
70. A. Arbuzov, D. Bardin, S. Bondarenko, P. Christova, L. Kalinovskaya, G. Nanava, and R. Sadykov. One-loop corrections to the Drell-Yan process in SANC. I. The Charged current case. *Eur. Phys. J. C*, 46:407–412, 2006. [Erratum: *Eur.Phys.J.C* 50, 505 (2007)].
71. C. M. Carloni Calame, G. Montagna, O. Nicrosini, and A. Vicini. Precision electroweak calculation of the charged current Drell-Yan process. *JHEP*, 12:016, 2006.
72. V. A. Zykunov. Weak radiative corrections to Drell-Yan process for large invariant mass of di-lepton pair. *Phys. Rev. D*, 75:073019, 2007.
73. C. M. Carloni Calame, G. Montagna, O. Nicrosini, and A. Vicini. Precision electroweak calculation of the production of a high transverse-momentum lepton pair at hadron colliders. *JHEP*, 10:109, 2007.
74. A. Arbuzov, D. Bardin, S. Bondarenko, P. Christova, L. Kalinovskaya, G. Nanava, and R. Sadykov. One-loop corrections to the Drell-Yan process in SANC. (II). The Neutral current case. *Eur. Phys. J. C*, 54:451–460, 2008.
75. Stefan Dittmaier and Max Huber. Radiative corrections to the neutral-current Drell-Yan process in the Standard Model and its minimal supersymmetric extension. *JHEP*, 01:060, 2010.
76. Roberto Bonciani, Federico Buccioni, Narayan Rana, and Alessandro Vicini. Next-to-Next-to-Leading Order Mixed QCD-Electroweak Corrections to on-Shell Z Production. *Phys. Rev. Lett.*, 125(23):232004, 2020.
77. Roberto Bonciani, Luca Buonocore, Massimiliano Grazzini, Stefan Kallweit, Narayan Rana, Francesco Tramontano, and Alessandro Vicini. Mixed Strong-Electroweak Corrections to the Drell-Yan Process. *Phys. Rev. Lett.*, 128(1):012002, 2022.
78. Tommaso Armadillo, Roberto Bonciani, Simone Devoto, Narayan Rana, and Alessandro Vicini. Two-loop mixed QCD-EW corrections to neutral current Drell-Yan. *JHEP*, 05:072, 2022.

79. Nikolaos Kidonakis and George Sterman. Subleading logarithms in qcd hard scattering. *Phys. Lett. B*, 387:867–874, 1996.
80. S. Moch and A. Vogt. On non-singlet physical evolution kernels and large-x coefficient functions in perturbative QCD. *JHEP*, 11:099, 2009.
81. G. Soar, S. Moch, J. A. M. Vermaseren, and A. Vogt. On Higgs-exchange DIS, physical evolution kernels and fourth-order splitting functions at large x. *Nucl. Phys. B*, 832:152–227, 2010.
82. D. Bonocore, E. Laenen, L. Magnea, S. Melville, L. Vernazza, and C. D. White. A factorization approach to next-to-leading-power threshold logarithms. *JHEP*, 06:008, 2015.
83. V. Del Duca, E. Laenen, L. Magnea, L. Vernazza, and C. D. White. Universality of next-to-leading power threshold effects for colourless final states in hadronic collisions. *JHEP*, 11:057, 2017.
84. Martin Beneke, Alessandro Broggio, Mathias Garny, Sebastian Jaskiewicz, Robert Szafron, Leonardo Vernazza, and Jian Wang. Leading-logarithmic threshold resummation of the Drell-Yan process at next-to-leading power. *JHEP*, 03:043, 2019.
85. N. Bahjat-Abbas, D. Bonocore, J. Sinninghe Damsté, E. Laenen, L. Magnea, L. Vernazza, and C. D. White. Diagrammatic resummation of leading-logarithmic threshold effects at next-to-leading power. *JHEP*, 11:002, 2019.
86. Martin Beneke, Alessandro Broggio, Sebastian Jaskiewicz, and Leonardo Vernazza. Threshold factorization of the Drell-Yan process at next-to-leading power. *JHEP*, 07:078, 2020.
87. Martin Beneke, Mathias Garny, Sebastian Jaskiewicz, Robert Szafron, Leonardo Vernazza, and Jian Wang. Leading-logarithmic threshold resummation of Higgs production in gluon fusion at next-to-leading power. *JHEP*, 01:094, 2020.
88. Ian Moult, Iain W. Stewart, and Gherardo Vita. Subleading Power Factorization with Radiative Functions. *JHEP*, 11:153, 2019.
89. Ze Long Liu, Bianka Mecaj, Matthias Neubert, and Xing Wang. Factorization at subleading power, Sudakov resummation, and endpoint divergences in soft-collinear effective theory. *Phys. Rev. D*, 104(1):014004, 2021.
90. Melissa van Beekveld, Wim Beenakker, Rahul Basu, Eric Laenen, Anuradha Misra, and Patrick Motylinski. Next-to-leading power threshold effects for resummed prompt photon production. *Phys. Rev. D*, 100(5):056009, 2019.
91. G. Das, S. Moch, and A. Vogt. Approximate four-loop QCD corrections to the Higgs-boson production cross section. *Phys. Lett. B*, 807:135546, 2020.
92. Ajjath A H, Pooja Mukherjee, and V. Ravindran. Next to soft corrections to Drell-Yan and Higgs boson productions. *Phys. Rev. D*, 105(9):094035, 2022.
93. Ajjath A H, Pooja Mukherjee, V. Ravindran, Aparna Sankar, and Surabhi Tiwari. Resummed Higgs boson cross section at next-to SV to NNLO + $\overline{\text{NNLL}}$. *Eur. Phys. J. C*, 82(9):774, 2022.
94. Melissa van Beekveld, Eric Laenen, Jort Sinninghe Damsté, and Leonardo Vernazza. Next-to-leading power threshold corrections for finite order and resummed colour-singlet cross sections. *JHEP*, 05:114, 2021.
95. Ajjath A H, Pooja Mukherjee, and V. Ravindran. Going beyond soft plus virtual. *Phys. Rev. D*, 105(9):L091503, 2022.
96. M. Beneke, M. Garny, S. Jaskiewicz, J. Strohm, R. Szafron, L. Vernazza, and J. Wang. Next-to-leading power endpoint factorization and resummation for off-diagonal “gluon” thrust. *JHEP*, 07:144, 2022.
97. Ze Long Liu, Matthias Neubert, Marvin Schnubel, and Xing Wang. Factorization at next-to-leading power and endpoint divergences in $gg \rightarrow h$ production. *JHEP*, 06:183, 2023.
98. George Sterman and Werner Vogelsang. Power corrections to electroweak boson production from threshold resummation. *Phys. Rev. D*, 107(1):014009, 2023.
99. Sourav Pal and Satyajit Seth. On Higgs+jet production at next-to-leading power accuracy. *Phys. Rev. D*, 109(11):114018, 2024.

100. Goutam Das and Aparna Sankar. Next-to-soft threshold effects on Higgs boson production via bottom quark annihilation. 9 2024.
101. Stefano Catani, Michelangelo L. Mangano, Paolo Nason, and Luca Trentadue. The Resummation of soft gluons in hadronic collisions. Nucl. Phys. B, 478:273–310, 1996.
102. S. Bailey, T. Cridge, L. A. Harland-Lang, A. D. Martin, and R. S. Thorne. Parton distributions from LHC, HERA, Tevatron and fixed target data: MSHT20 PDFs. Eur. Phys. J. C, 81(4):341, 2021.
103. Andy Buckley, James Ferrando, Stephen Lloyd, Karl Nordström, Ben Page, Martin Rufenacht, Marek Schönherr, and Graeme Watt. LHAPDF6: parton density access in the LHC precision era. Eur. Phys. J. C, 75:132, 2015.
104. Charalampos Anastasiou, Claude Duhr, Falko Dulat, Bernhard Mistlberger, and Konstantin U. Schönwald. High precision QCD at high energies. Phys. Rev. Lett., 121(16):162001, 2018.
105. Julien Baglio, Claude Duhr, Bernhard Mistlberger, and Robert Szafron. Inclusive Production Cross Sections at N3LO. 9 2022.
106. Stefano Forte and Claudio Muselli. High-energy resummation of Drell-Yan processes. JHEP, 03:122, 2016.
107. Radja Boughezal, Christoph Focke, Xiaohui Liu, and Frank Petriello. Next-to-leading-logarithmic power corrections for Higgs boson production in association with a vector boson. Phys. Rev. Lett., 115(6):062002, 2016.
108. Ajjath A H, Pooja Mukherjee, V. Ravindran, Aparna Sankar, and Surabhi Tiwari. Next-to SV resummed Drell-Yan cross section beyond leading-logarithm. Eur. Phys. J. C, 82(3):234, 2022.
109. Leonardo Vernazza. Factorization and resummation at next-to-leading-power. PoS, RADCOR2023:050, 2024.
110. Alessandro Broggio, Sebastian Jaskiewicz, and Leonardo Vernazza. Threshold factorization of the Drell-Yan quark-gluon channel and two-loop soft function at next-to-leading power. JHEP, 12:028, 2023.
111. Ajjath A H, Pooja Mukherjee, V. Ravindran, Aparna Sankar, and Surabhi Tiwari. Next-to-soft corrections for Drell-Yan and Higgs boson rapidity distributions beyond N³LO. Phys. Rev. D, 103:L111502, 2021.
112. Ajjath A H, Pooja Mukherjee, V. Ravindran, Aparna Sankar, and Surabhi Tiwari. Next-to-soft-virtual resummed rapidity distribution for the Drell-Yan process to NNLO+NNLL⁻. Phys. Rev. D, 106(3):034005, 2022. [Erratum: Phys.Rev.D 108, 019901 (2023)].